Small Reorganization Energy of Intramolecular Electron Transfer in Fullerene-Based Dyads with Short Linkage

Kei Ohkubo,[†,‡] Hiroshi Imahori,*[,§] Jianguo Shao,[||] Zhongping Ou,[||] Karl M. Kadish,*[,||] Yihui Chen,[⊥] Gang Zheng,[⊥] Ravindra K. Pandey,*[,⊥,#] Mamoru Fujitsuka,[@] Osamu Ito,*[,@] and Shunichi Fukuzumi*[,†]

Department of Material and Life Science, Graduate School of Engineering, Osaka University, CREST, Japan, Science and Technology Corporation, Suita, Osaka 565-0871, Japan, Department of Molecular Engineering, Graduate School of Engineering, Kyoto University, PRESTO, JST, Kyoto 606-8501, Japan, Department of Chemistry, University of Houston, Houston, Texas 77204-5003, Chemistry Division, Photodynamic Therapy Center, Roswell Park Cancer Institute, Buffalo, New York, 14263, Department of Nuclear Medicine, Roswell Park Cancer Institute, Buffalo, New York, 14263, and Institute of Multidisciplinary Research for Advanced Materials, Tohoku University, CREST, JST, Sendai, Miyagi, 980-8577, Japan

Received: July 25, 2002; In Final Form: September 16, 2002

A bacteriochlorin-C_{60} dyad (H_2BCh-C_{60}) and a zinc chlorin dyad (ZnCh-C_{60}) with the same short spacer have been synthesized. The rate constants for the charge-separation (CS) processes in these dyads were determined by fluorescence lifetime measurements of the dyads. The charge-recombination (CR) rate constants of the dyads were determined using laser flash photolysis. The photoexcitation of the zinc chlorin-C_{60} dyad results in formation of the long-lived radical ion pair, which has absorption maxima at 790 and 1000 nm due to the zinc chlorin radical cation and the C_{60} radical anion, respectively. Photoexcitation of the free-base bacteriochlorin-C_{60} dyad with the same short linkage leads to formation of the radical ion pair, which decays quickly to the triplet excited state of the bacteriochlorin moiety. The driving force dependence of the electron-transfer rate constants of these dyads with a short spacer affords a small reorganization energy ($\lambda = 0.51$ eV) as compared with the λ value (0.66 eV) of zinc porphyrin-C_{60} dyads with a longer spacer.

Introduction

Extensive efforts have been devoted toward the preparation of electron donor−acceptor linked compounds which, upon photoexcitation, give rise to a long-lived photoinduced charge-separated state in high quantum yields as achieved in the photosynthetic reaction center.[1−9] Porphyrins that have highly delocalized π systems are suitable for efficient electron transfer because the uptake or release of electrons results in minimal structural and solvation changes upon electron transfer.[4,9] A long-lived photoinduced charge-separated state exhibiting a lifetime of milliseconds was observed by using a chlorophyll−porphyrin−quinone triad.[10] In this case, however, a significant amount of energy was lost during the sequential electron transfer. With the advent of fullerenes, a new three-dimensional electron acceptor became available, exhibiting attractive characteristics.[1,5,7] In particular, fullerenes have remarkably small reorganization energies of electron transfer, which result from the π-electron systems being delocalized over the three-dimensional surface together with the rigid, confined structure of the aromatic π sphere.[12−14] The small reorganization energy leads to acceleration of the charge separation (CS) and deceleration of the charge recombination (CR) processes as expected from the Marcus theory of electron transfer.[15] The rate of CR can be markedly slowed by shifting deep into the inverted region of the Marcus parabola where the driving force ($-\Delta G^0_{ET}$) is larger than the total reorganization energy (λ) of electron transfer.[15] Extensive efforts have been directed toward establishing the driving force dependence of rate constants for the electron transfer and thereby probing the Marcus inverted region where the electron-transfer rate decreases with increasing the driving force of electron transfer.[12−14] We have recently achieved a 380 ms charge-separated lifetime by using a ferrocene−porphyrin−porphyrin−C_{60} tetrad.[16] In natural systems, however, reduced porphyrins, namely chlorins and bacteriochlorins, are the electron donor pigments of the electron-transfer processes. The number of reduced double bonds in the pyrrole rings is zero in the case of porphyrins, one in the case of chlorins, and two diagonal to each other in the case of bacteriochlorins. This difference in the degree of macrocycle conjugation leads to a considerable change in the excited states, absorption spectra, and redox properties.[17−19] Therefore, it is of great interest to examine the use of chlorophyll-like molecules such as chlorins.[17−19] Some researchers have previously reported the synthesis and photochemical and electrochemical properties of a chlorophyll-like donor (a chlorin) linked to C_{60} (chlorin-C_{60}) or porphyrin-C_{60} dyads with the same short spacer between the macrocycle and the fullerene.[20−22] The photoexcitation of the zinc chlorin-C_{60} dyad results in an unusually long-lived radical ion pair.[23] However, bacteriochlorin-C_{60} as a bacterichlorophyll-like donor linked fullerene dyad has not been reported.

In the present study, we have designed and synthesized new free-base bacteriochlorin- and zinc chlorin-fullerene dyads.

* Corresponding authors. E-mail addresses: fukuzumi@ap.chem.eng.osaka-u.ac.jp; imahori@mee3.moleng.kyoto-u.ac.jp; Ravindra.Pandey@RoswellPark.org; KKadish@uh.edu; ito@tagen.tohoku.ac.jp.
† Osaka University.
‡ Science and Technology Corporation.
§ Kyoto University.
|| University of Houston.
⊥ Photodynamic Therapy Center, Roswell Park Cancer Institute.
Department of Nuclear Medicine, Roswell Park Cancer Institute.
@ Tohoku University.

10.1021/jp026603+ CCC: $22.00
Published on Web 10/23/2002

CHART 1

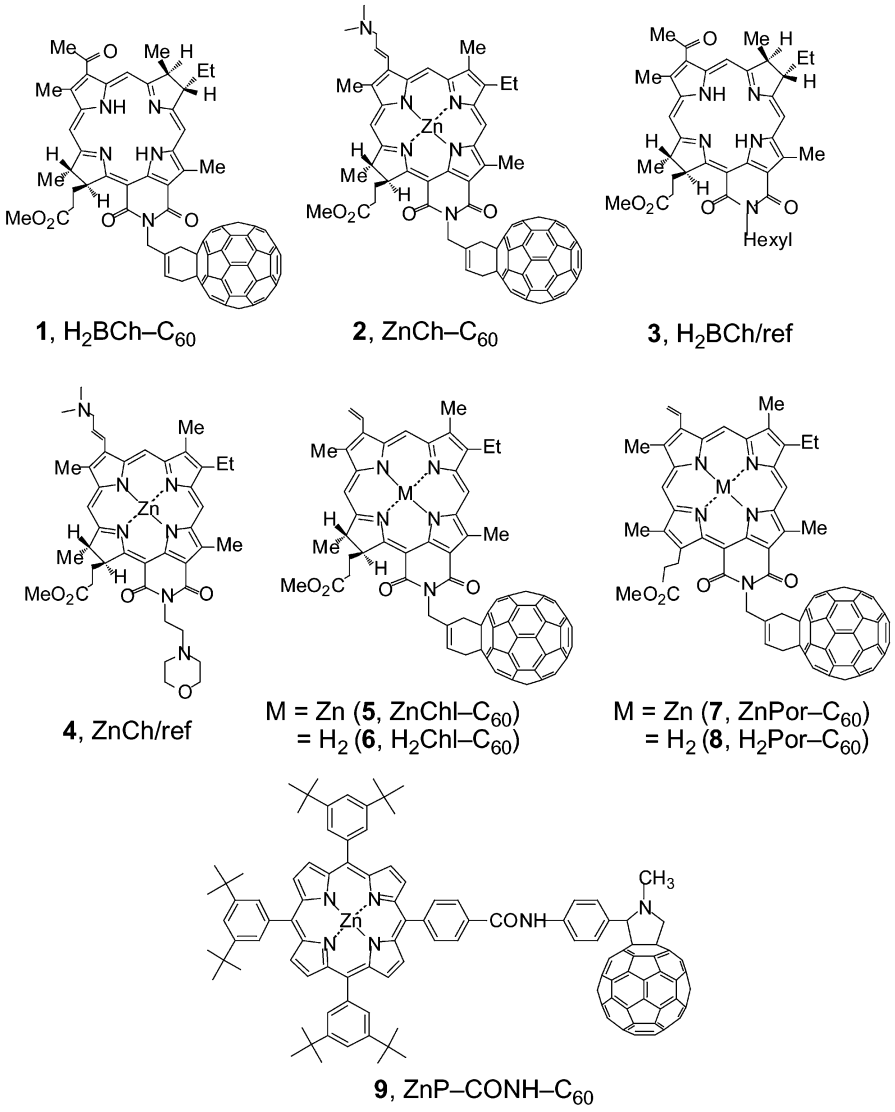

These dyads (**1** and **2**) and their reference compounds (**3** and **4**) are shown in Chart 1, together with the related dyads reported previously (**5**−**9**).[14,23] The dyads (**1**, **2**, **5**−**8**) contain the same short spacer, where the edge-to-edge distance (R_{ee}) is 5.9 Å. This is significantly shorter than the R_{ee} value (11.9 Å) of ZnP−CONH−C_{60} (**9**).[14] The electrochemical and photochemical properties of these dyads have been investigated in detail. These data, together with those of similar dyads with a longer spacer reported earlier, provide an excellent opportunity to examine the effects of spacer distance on the rates of photoinduced electron transfer and back electron transfer of these dyads in light of the Marcus theory of electron transfer.

Experimental Section

General. Tetrabutylammonium perchlorate (*n*-Bu_4NClO_4), used as a supporting electrolyte for the electrochemical measurements was obtained from Fluka Fine Chemicals, recrystallized from ethanol and dried in vacuo prior to use. Benzonitrile was purchased from Wako Pure Chemical Ind., Ltd. and purified by successive distillation over P_2O_5.[24]

Time-resolved spectroscopic, electrochemical, and ESR measurements of the dyads were perfomed as reported previously.[23]

Synthesis. The dyads were synthesized by following the reaction sequences as shown in Schemes 1 and 2.

*Bacteriopurpurin-18-N-propargylimide methyl ester (**11**).* A mixture of bacteriopurpurin-18 methyl ester **10** (80 mg, 0.13 mmol) and propargylamine (2 g, 36 mmol) in 30 mL benzene was refluxed overnight under an argon atmosphere, after which solvent and excess reagent were removed. The crude product thus obtained was chromatographed on silica column, eluting with 2% MeOH/CH_2Cl_2. After evaporating the solvents, **11** was obtained in 60% yield (50 mg), mp 244 °C. FAB for $C_{37}H_{39}N_5O_5$ (*m*/*z*): 633.5 (M^+). HRMS calcd 634.3023 (M + 1); found 634.3035. UV−vis [CH_2Cl_2, nm(ϵ)]: 365 (8.9×10^4), 415 (4.4×10^4), 545 (3.3×10^4), 755 (1.7×10^4), 825 (6.4×10^4). ^{1}H NMR (400 MHz, 5.0 mg/mL $CDCl_3$, δ ppm): 9.22, 8.81, and 8.62 (each s, 1H, 5-H, 10-H, and 20-H), 5.32 (m, J = 7.3 Hz, 1H, 17-H), 5.25 (dd, 2H, J = 6.6, 2.2 Hz, *N*-CH_2), 4.31 (m, 1H, 17-H), 4.28 (q, J = 7.7 Hz, 1H, 18-H), 4.10 (m, 1H, 8-H), 3.72, 3.59, 3.55, and 3.18 (each s, 3H, 2- CH_3, 12-CH_3, CO_2CH_3 and $COCH_3$), 2.71, 2.36, 2.08, and 1.96 (each m, 1H, 17^1-CH_2 and 17^2-CH_2), 2.40 (q, J = 10.3 Hz, 2H, 8-*CH*$_2$$CH_3$), 2.30 (t, J = 2.2 Hz, 1H, CH), 1.83 and 1.72 (each d, J = 7.5 Hz, 3H, 7-CH_3 and 18-CH_3), 1.12 (t, J = 7.2 Hz, 3H, 8-CH_2*CH*$_3$), −0.40 and −0.64 (each br s, 1H, 2 x N−H).

*Bacteriochlorin-diene (**12**).* To a solution of **11** (70 mg, 0.11 mmol) in 10 mL dichloromethane was added 10 mg of Grubbs' catalyst (10 mol %). The reaction mixture was stirred under

SCHEME 1

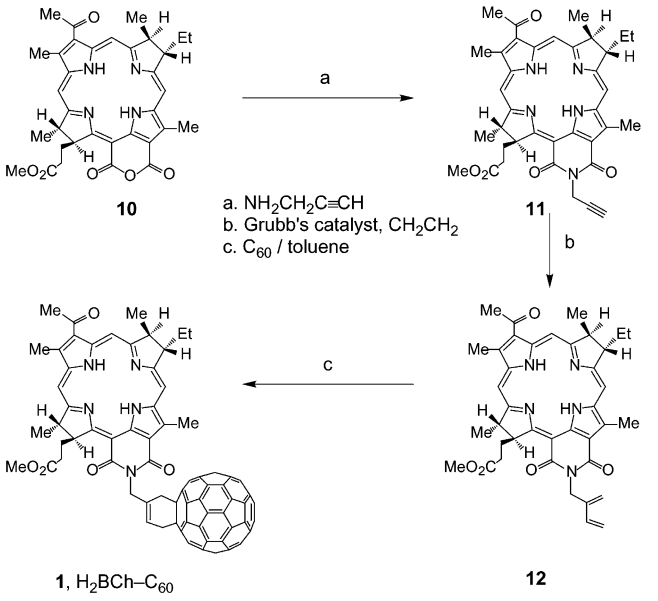

ethylene gas balloon at room temperature for 48 h. After removing the solvent, the crude product was chromatographed on silica plate, eluting with 2% MeOH/CH_2Cl_2, and **12** was obtained in a 50% yield (35 mg), along with 30% (20 mg, 0.03 mmol) of the starting material, mp 268 °C. FAB calcd for $C_{39}H_{43}N_5O_5$ MS (*m*/*z*): 662.4 (M + 1). HRMS 662.3336 (M + 1); found 662.3346. UV−vis (CH_2Cl_2, nm(ϵ)): 365 (9.4×10^4), 415 (4.9×10^4), 545 (3.8×10^4), 825 (7.6×10^4). ^{1}H NMR (400 MHz, $CDCl_3$, δ ppm): 9.24, 8.83 and 8.64 (each s, 1H, 5-H, 10-H and 20-H), 6.67 (dd, J = 18.3 Hz, 11.8 Hz, 1H, diene-H), 5.60 (d, J = 18.3 Hz, 1H, diene-H), 5.33 (m, 1H, 17-H), 5.29 (d, J = 13.7 Hz, 1H, diene-H), 5.27 (s, 2H, N−CH_2), 5.17 (d, J = 24.3 Hz, 2H, diene-H), 4.31 (m, 1H, 7-H), 4.27 (q, J = 7.4 Hz, 1H, 18-H), 4.15 (dt, J = 8.2, 3.5 Hz, 1H, 8-H), 3.71 and 3.18 (each s, 3H, 2 × CH_3), 3.56 (s, 6H, 2 × CH_3), 2.67, 2.39, 2.08, and 1.96 (each m, 1H, 17^1-CH_2 and 17^2-CH_2), 2.36 (q, J = 10.2 Hz, 2H, 8-CH_2CH_3), 1.82 and 1.74 (each d, J = 7.5 Hz, 3H, 7-CH_3 and 18-CH_3), 1.12 (t, J = 7.2 Hz, 3H, 8-CH_2CH_3), −0.42 and −0.67 (each br s, 1H, 2 × N−H).

*Bacteriochlorin-C_{60} Dyad (**1**, H_2BCh-C_{60}).* Diene **12** (27 mg, 0.041 mmol) and C_{60} (30 mg, 0.042 mmol) were mixed in 20 mL toluene and refluxed for 2 h under argon. After removing the solvent, the crude products were chromatographed on silica plate, eluting with 2% MeOH/CH_2Cl_2, and the desired product **1** was obtained in 28% yield (16 mg). Melting point: >300 °C. UV−vis [CH_2Cl_2, nm (ϵ)]: 365 (9.7×10^4), 415 (4.5×10^4), 550 (3.6×10^4), 830 (7.1×10^4). FAB calculated for $C_{99}H_{43}N_5O_5$ (*m*/*z*): 1382.6 (M + 1), 720.7 (C_{60}). HRMS calcd 1382.3336 (M + 1); found 1382.3358. ^{1}H NMR (400 MHz, 5.0 mg/mL $CDCl_3$, δ ppm): 9.18, 8.69, and 8.55 (each s, 1H, 5-H, 10-H and 20-H), 7.23 (t, J = 6.9 Hz, 1H, cyclohexene-H), 5.66 (ABX, J = 22.1, 14.0 Hz, 2H, *N*-CH_2), 5.22 (m, J = 8.9 Hz, 1H, 17-H), 4.32 (ABX, J = 14.4, 12.4 Hz, 2H, cyclohexene-H), 4.26 (m, J = 6.9, 3.4 Hz, 1H, 7-H), 4.21 (q, J = 7.2 Hz, 1H, 18-H), 4.06 (dt, J = 8.2, 3.5 Hz, 1H, 8-H), 3.98 (d, J = 6.0 Hz, 2H, cyclohexene-H), 3.64, 3.54, 3.51, and 3.16 (each s, 3H, 4 × CH_3), 2.39 (q, J = 7.5 Hz, 2H, 8CH_2-CH_3), 2.69, 2.30, 2.03, and 1.85 (each m, 1H, 17^1-CH_2 and 17^2-CH_2), 1.81 and 1.61 (each d, J = 7.2 Hz, 3H, 7-CH_3 and 18-CH_3), 1.06 (t, J = 7.5 Hz, 3H, 8-CH_2CH_3), −0.56 and −0.69 (each br s, 1H, 2 × N−H).

*Purpurin-18-N-(2-morpholine)ethylene-imide Methyl Ester (**14**).* Purpurin-18 methyl ester **13** (100 mg, 0.17 mmol) was reacted with 4-(2-aminoethyl)morpholine (1 mL, 7.6 mmol) by following the procedure described for the preparation of **11**,

SCHEME 2

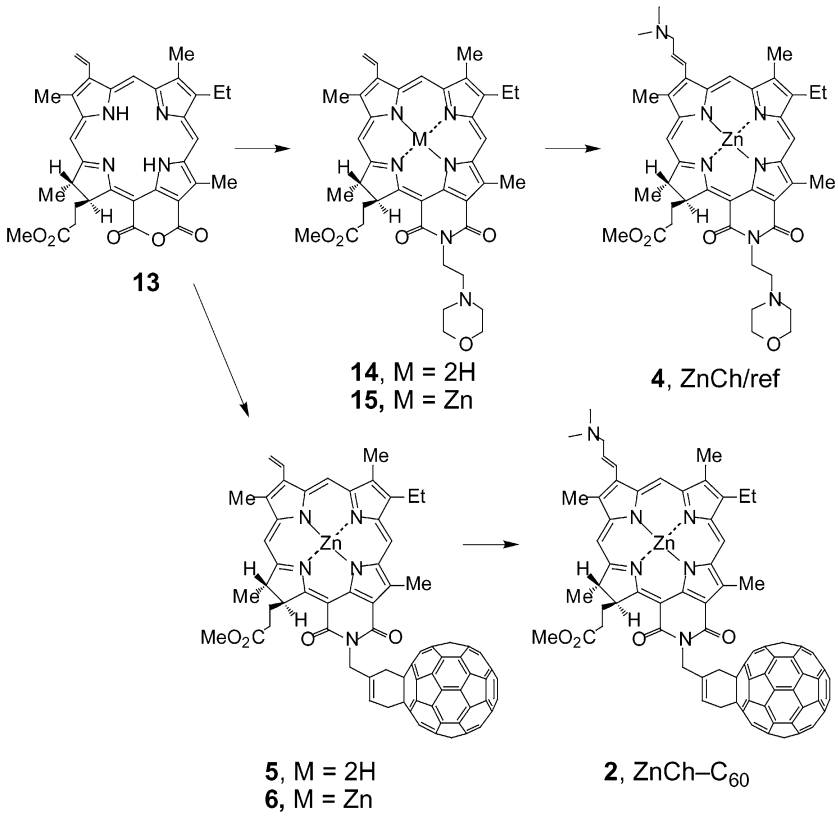

and the desired imide analogue was obtained in 72% (84.5 mg) yield, mp. 120 °C. UV−vis [CH_2Cl_2, nm (ϵ)]: 365 (5.4×10^4), 420 (1.4×10^5), 485 (5.4×10^3), 510 (7.7×10^3), 550 (2.5×10^4), 650 (9.0×10^3), 705 (5.4×10^4). Mass calcd. for $C_{40}H_{46}N_6O_5$ 690.35; found (FAB) *m/z* 691.8 (M + 1). Analysis calcd for $C_{40}H_{46}N_6O_5 \cdot 1/2H_2O$: C, 68.63; H, 6.77; N, 12.01. Found: C, 68.76; H, 6.73; N, 11.62. ^{1}H NMR ($CDCl_3$, δ ppm): 9.62, 9.40, and 8.55 (each s, 1H, *meso*-H), 7.78 (dd, J = 18.6, 11.4 Hz, 1H, C*H*═CH_2), 6.26 and 6.12 (each d, 1H, CH═CH_2), 5.40 (d, 1H, J = 7.8 Hz, 18H), 4.60 (m, imide-*N*-CH_2), 4.37 (q, m, J = 6.7 Hz, 1H, 17H), 3.80, 3.55, 3.37, 3.12 (each s, 3H, $-CO_2CH_3$ and 2, 7, 12 $-CH_3$), 3.70 (br, 4H, morpholine O−CH_2), 2.80−1.80 (several peaks, 10H, $-CH_2CH_2$-CO_2CH_3 and $-CH_2CH_2-N-(CH_2)_2$ of morpholine), 1.75 (d, J = 7.18 Hz, 3H, 18-CH_3), 1.60 (t, J = 7.1 Hz, 3H, 8-CH_2-CH_3), 0.05 and 0.08 (each s, 1H, 2 × NH).

*Zn(II) Purpurin-18-N-(2-morpholine)ethylene-imide Methyl Ester (**15**).* Purpurinimide **14** (50 mg, 0.072 mmol) was reacted with $Zn(OAc)_2$ in methanol by following the procedure described for Zn(II)imide **3**, and the title compound was isolated in 90% yield (48.8 mg): mp 169 °C. ^{1}H NMR ($CDCl_3$, δ ppm): 9.28, 9.12, and 8.30 (each s, 1H, *meso*-H), 7.80 (m, 1H, $-CH$═CH_2), 6.10 and 6.00 (each d, J = 7.3 and 11.5 Hz, respectively, 1H, CH═CH_2), 5.30 (br, 1H, 17-H), 4.20 (2H, m, imide-*N*-CH_2), 3.60 (m, 3H, 18-H and 8-CH_2CH_3), 3.55, 3.45, 3.20, and 3.10 (each s, 3H, CO_2CH_3 and 2× ring-CH_3 and −O−$(CH_2)_2$ of morpholine; 2.65 (s, 3H, N−$(CH_3)_2$, 2.60 (3H, ring-CH_3), 2.80−1.80 (several peaks, 10H, $-CH_2CH_2CO_2CH_3$,-$CH_2CH_2-N-(CH_2)_2$ of morpholine), 1.75 (brt, J = 8.0 Hz, 3H, 18-CH_3), 1.62 (brs, 3H, 8-CH_2CH_3), 1.20 (brs, 2H, 2 × NH).

Zinc(II) 3-Devinyl-3-[2-(N,N-dimethylamino)]prop-1-enyl-purpurin-18-N−(2-morpholine)-ethyleneimide Methyl Ester (***4***, *ZnCh/ref).* To a solution of purpurinimide (**15**) (40 mg, 0.053 mmol) in 20 mL dichloromethane was added Eschenmoser's salt (*N,N*-dimethylmethyleneammonium iodide) (250 mg, 13.5 mmol). The reaction mixture was stirred at room temperature under argon overnight. After the standard workup, the crude product was chromatographed on an alumina (Gr III) column, eluting with 10% MeOH in CH_2Cl_2. Compound **4** was obtained in 60% yield (25.7 mg), mp. 240 °C. UV−vis [CH_2Cl_2, nm (ϵ)]: 434 (6.5×10^4), 524 (2.0×10^3), 569 (6.6×10^3), 635 (9.0×10^3), 683 (3.6×10^4). Mass calcd. for $C_{43}H_{51}N_7O_5Zn$ 809.32; found (FAB) *m/z* 811.3 (M + 2). HRMS calcd (M + 1) 810.3312; found 810.3292. ^{1}H NMR ($CDCl_3$, δ ppm): 9.50, 8.35, and 8.12 (each s, 1H, *meso*-H), 6.00 and 5.40 (each br, 1H, C*H*═CH), 4.60 (br, 2H, imide-*N*-CH_2), 4.35 (brm, 2H, 17- and 18-H), 3.70−3.75 (several peaks merged, 11H, CO_2CH_3, 2 × ring CH_3 and 8-CH_2CH_3), 3.62 (m, 2H, $-CH_2N(CH_3)_2$), 3.00−2.5 (several peaks, 12H), 2.60−1.80 (several peaks, 10H, $-CH_2CH_2CO_2CH_3$, $-CH_2CH_2-N-(CH_2)_2$ of morpholine), 1.80 (m, 6H, 18-CH_3 and 8-CH_2CH_3).

*Zn(II) 3-Devinyl-3-[2-(N,N-dimethylamino)prop-1-enyl-purpurin-18-N−C60 Imide (**2**, ZnCh-C60).* Purpurinimide-C_{60} conjugate (**6**, 36 mg, 0.025 mmol)[23] was reacted with Eschenmoser's salt (300 mg, 1.61 mmol) by following the procedure described for the foregoing purpurinimide and the title compound was isolated in 60% yield (22 mg, 0.015 mmol). FAB for $C_{102}H_{46}N_6O_4Zn$ (*m/z*): 1483.3 (M + 1). HRMS calcd 1483.2942 (M + 1); found 1483.2987. UV−vis [CH_2Cl_2, nm(ϵ)]: 434 (7.2×10^4), 521 (3.6×10^3), 572 (8.3×10^3), 638 (1.1×10^4), 689 (3.7×10^4). ^{1}H NMR (400 MHz, 5.0 mg/mL $CDCl_3$, δ ppm) all resonances were observed as broad peaks possibly due to strong aggregation.

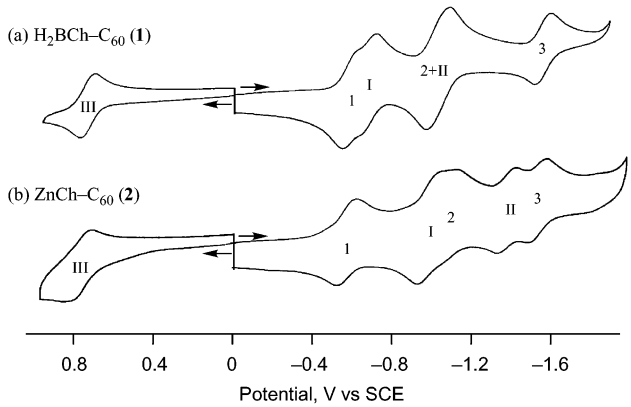

Figure 1. Cyclic voltammograms of (a) **1** and (b) **2** in the presence of 0.10 M *n*-Bu_4NClO_4 in PhCN.

TABLE 1: Half-wave Potentials (V vs SCE) of Dyads and Reference Compounds in PhCN Containing 0.1 M TBAP

	oxidation	reduction				
compound	1st	1st	2nd	3rd	4th	5th
H_2BCh-C_{60} (**1**)	0.76	−0.59	−0.70	−1.05[a]	−1.05[a]	−1.59
ZnCh-C_{60} (**2**)	0.78	−0.58	−0.99	−1.11	−1.40	−1.55
H_2BCh/ref (**3**)	0.75		−0.63	−1.04		
ZnCh/ref (**4**)	0.75			−1.15	−1.43	

[a] Two overlapped one-electron processes.

Results and Discussion

Synthesis and Characterization. H_2BCh-C_{60} (**1**) and ZnCh-C_{60} (**2**) dyads (Chart 1) were synthesized via a Diels−Alder reaction of the chlorin and porphyrin with the fullerene (see Experimental Section).[21,22] These tetrapyrrolic compounds contain a six-membered fused imide ring system and present an opportunity to design fullerene conjugates containing a spacer with a defined length and geometry. The ^{1}H NMR spectra of the dyads revealed the presence of only a single species in solution (see Experimental Section).

The absorption spectra of **1** and **2** in benzonitrile (PhCN) are reasonable superpositions of the spectra of the component chromophores making up these molecules. Thus, there is no significant electronic interaction between the individual chromophores in their ground-state configuration.

Electrochemical Properties. The cyclic voltammograms of H_2BCh-C_{60} (**1**) and ZnCh-C_{60} (**2**) are shown in Figure 1, while the half-wave potentials ($E_{1/2}$) of these complexes together with those of unlinked H_2BCh/ref (**3**) and ZnCh/ref (**4**) without C_{60} are summarized in Table 1.[25] A comparison with the unlinked compounds (**3** and **4**) reveals that the cyclic voltammograms of **1** and **2** consist of three one-electron reduction processes of C_{60}, two one-electron reduction processes of the macrocyclic ring and a single one-electron oxidation process. The first one-electron reduction of **1** occurs at the C_{60} site at $E_{1/2}$ (vs SCE) of −0.59 V, and the second one-electron reduction occurs at the H_2BCh site at a slightly more negative potential (−0.70 V). The second one-electron reduction of $C_{60}^{\bullet -}$ is overlapped with the second one-electron reduction of $H_2BCh^{\bullet -}$ at −1.05 V (Figure 1a). The one-electron reduction of C_{60}^{2-} is observed at −1.59 V (Figure 1a). The first one-electron reduction of **2** also occurs at the C_{60} site at $E_{1/2}$ = −0.58 V (Figure 1b) which is nearly the same as the value of **1** (−0.59 V). In this case, the one-electron reduction of ZnCh occurs at a more negative potential (−0.99 V) as compared to the value of **1** (−0.70 V). The one-electron reduction of $C_{60}^{\bullet -}$, $ZnCh^{\bullet -}$, and C_{60}^{2-} occurs at −1.11 V, −1.40 V, and −1.55 V, respectively (Figure 1b).

TABLE 2: Rate Constants of ET and BET (k_{ET} and k_{BET}), Triplet Decay Rate Constants (k_T), and Driving Force ($-\Delta G^0_{ET}$ and $-\Delta G^0_{BET}$)

no.	excited state[a]	$-\Delta G^0_{ET}$ (eV)	k_{ET} (s^{-1})	$-\Delta G^0_{BET}$ (eV)	k_{BET} (s^{-1})	k_T (s^{-1})
1	$^1H_2BCh^*$-C_{60} (**1**)	0.10	2.5×10^9	1.35		1.5×10^4
2	$^1ZnCh^*$-C_{60} (**2**)	0.41	1.8×10^{10}	1.36	2.0×10^4	
3	$^1ZnChl^*$-C_{60} (**5**)	0.46	2.4×10^{10}	1.33	9.1×10^3	
4	$^1H_2Chl^*$-C_{60} (**6**)	0.17	4.1×10^9	1.57		1.5×10^4
5	$^1ZnPor^*$-C_{60} (**7**)	0.33	7.4×10^9	1.51		2.0×10^4
6	$^1H_2Por^*$-C_{60} (**8**)	0.11	6.6×10^8	1.72		4.6×10^4

[a] The data of **5**−**8** are taken from ref 23.

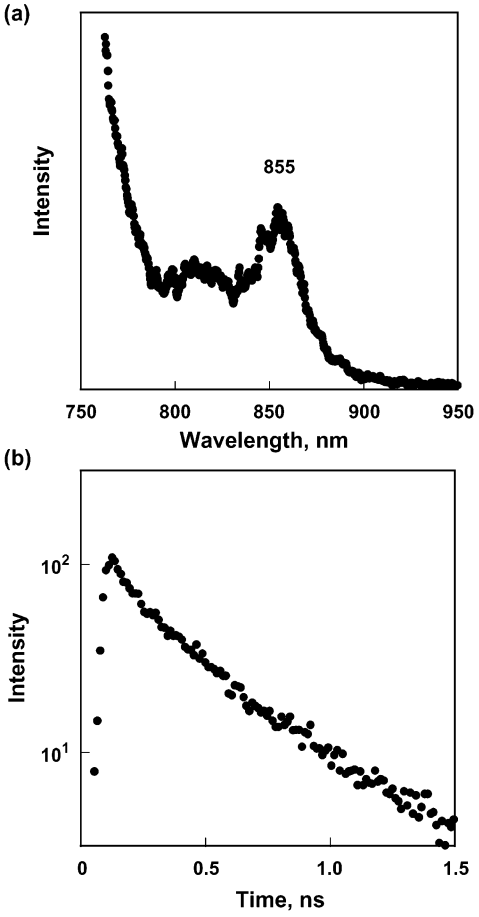

Figure 2. (a) Fluorescence spectrum of H_2BCh-C_{60} (**1**) in deaerated PhCN solution accumulated from 0 to 1.0 ns after laser excitation (λ = 410 nm) at 298 K. (b) Time profile of fluorescence at 855 nm.

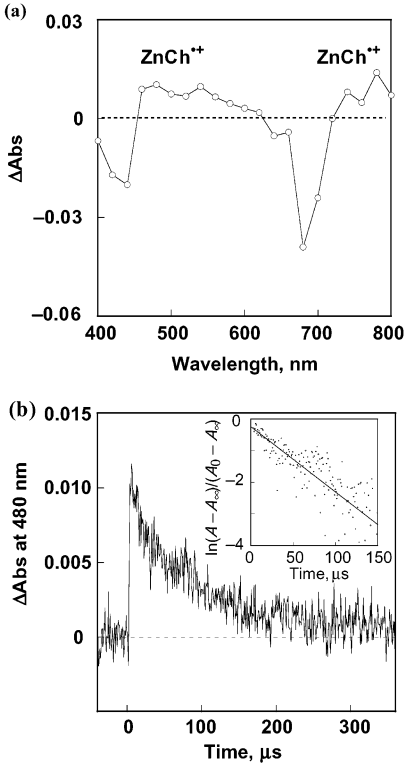

Figure 3. (a) Transient absorption spectrum of ZnCh-C_{60} (**2**) (1.0×10^{-4} M) in deaerated PhCN at 298 K taken at 0.1 μs after laser excitation at 355 nm, (b) the decay profile at 480 nm. Inset: First-order plot.

On the other hand, the one-electron oxidation of **1** and **2** occurs at the macrocyclic ring at 0.76 and 0.78 V, respectively. The one-electron oxidation of C_{60} is known to be difficult as compared to the one-electron oxidation of macrocyclic ring.[26] Thus, in each case, the first one-electron oxidation and reduction occur at the macrocyclic ring and the C_{60} moiety, respectively.

Fluorescence Quenching. A deoxygenated PhCN solution containing H_2BCh-C_{60} (**1**) gives rise upon the photoexcitation with a 410 nm monochromatized light to a fluorescence spectrum with maximum at 855 nm as shown in Figure 2a.[27] The fluorescence decay was monitored at 855 nm due to the emission of the bacteriochlorin moiety.[19] The fluorescence emission from the C_{60} moiety could not be separated well from that from the bacteriochlorin moiety. The fluorescence decay curve at 855 nm was well-fitted by a single-exponential decay which is the major component as compared to the initial fast decay component (Figure 2b).[28] The fluorescence lifetime of the unlinked bacteriochlorin (τ(H_2BCh/ref (**3**)) = 1.2 ns)[19] was significantly reduced when it was replaced by **1** (τ(**1**) = 300 ps) due to electron transfer from the singlet excited state of H_2BCh ($^1H_2BCh^*$) to C_{60}. The rate constant of electron transfer (k_{ET}) from $^1H_2BCh^*$ to C_{60} is determined from the difference between τ(**1**)$^{-1}$ and τ(H_2BCh/ref)$^{-1}$ as 2.5×10^9 s^{-1}. Similarly, the k_{et} value of ZnCh-C_{60} (**2**) was determined as 1.8×10^{10} s^{-1} from the fluorescence lifetimes of ZnCh-C_{60} (**2**, τ = 56 ps) and ZnCh/ref (**4**, τ = 2.4 ns).

The free energy change of photoinduced electron transfer ($-\Delta G^0_{ET}$) from the $^1H_2BCh^*$ moiety to the C_{60} moiety in PhCN is determined to be −0.10 eV from the one-electron oxidation potential and the excitation energy (S_1 = 1.45 eV) of the H_2-BCh moiety and the one-electron reduction potential of the C_{60} moiety in **1** (Table 2).[29] The $-\Delta G^0_{ET}$ and rate constants of electron transfer are summarized in Table 2.

Detection of Intermediates in Photoinduced Electron Transfer. Upon a 355 nm laser light pulse irradiation, a deoxygenated PhCN solution containing ZnCh-C_{60} (**2**) gives rise to a transient absorption spectrum with maxima at 790 and 1000 nm as reported for the related system (see Supporting Information, S1). The transient absorption spectrum between 400 and 800 nm is shown in Figure 3a. The absorption band at 1000 nm (S1) is a clear attribute of the monofunctionalized fullerene radical anion.[23,30−32] The electrochemical oxidation of **2** in PhCN

containing 0.2 M *n*-Bu_4NClO_4 at an applied potential positive of the first reversible oxidation gives the chlorin π radical cation ($ZnCh^{\bullet+}$-C_{60}) whose spectrum has an absorption maximum at 790 nm.[23] The absorption band at 790 nm in Figure 3 agrees with that of the chlorin π-radical cation. Thus, the transient absorption spectrum in Figure 3 indicates formation of the radical ion pair state ($ZnCh^{\bullet+}$-$C_{60}^{\bullet-}$). The radical ion pair is lower in energy (1.36 eV) than both the triplet excited state of C_{60} (1.45 eV)[33] and ZnCh (1.45 eV).[23]

The radical ion pair detected in Figure 3a decays via back electron transfer (BET) to the ground-state rather than to the triplet excited state. The BET rate (k_{BET}) was determined from the disappearance of the absorption band at 480 nm due to $ZnCh^{\bullet+}$ in $ZnCh^{\bullet+}$-$C_{60}^{\bullet-}$ (Figure 3b). The decay of the absorption band obeys first-order kinetics (inset of Figure 3b). The k_{BET} value is determined as 2.0×10^4 s^{-1}.

Formation of such a long-lived radical ion pair state of $ZnCh^{\bullet+}$-$C_{60}^{\bullet-}$ enabled detection of the radical ion species produced by the photoinduced electron transfer in **2** with measurements of the ESR spectrum under photoirradiation of **2** as reported for the related system (see Supporting Information S2).[23] The ESR spectrum consists of two characteristic signals, one of which is attributable to an organofullerene radical anion at a small g value ($g = 2.0007$)[33] and the other to the chlorin radical cation at a higher g value ($g = 2.0031$).[23] Upon "turning off" the irradiation source, no significant decay of the ESR signal occurred for hours. This indicates that photoinduced electron transfer from ^{1}ZnCh* to C_{60} results in formation of the radical ion pair ($ZnCh^{\bullet+}$-$C_{60}^{\bullet-}$) and that an intermolecular electron transfer between radical ion pairs located close to each other in frozen PhCN occurs to give $ZnCh^{\bullet+}$-C_{60} and ZnCh-$C_{60}^{\bullet-}$, which are now separated from each other to prevent the BET.

In contrast to the case of ZnCh-C_{60} (**2**), no transient formation of $C_{60}^{\bullet-}$ was detected at 1000 nm for H_2BCh-C_{60} (**1**) as shown in Figure 4a and b. Instead, only the triplet−triplet absorption due to the bacteriochlorin moiety is observed due to the higher energy of the radical ion pair as compared to the triplet excited state, as is expected from the redox potentials (Figure 4b).[34] The decay of the triplet−triplet absorption at 440 nm obeys first-order kinetics (inset of Figure 4c). The triplet decay rate constant is determined as 1.5×10^4 s^{-1}, which agrees with the triplet decay rate constant of the reference compound (**3**).[19]

The fluorescence of **1** is efficiently quenched due to photoinduced electron transfer from $^1H_2$BCh* to C_{60} (vide supra). The main pathway is formation of the triplet state of the bacteriochlorin ($^3H_2$BCh*), since the triplet energy is lower than the radical ion pair ($H_2BCh^{\bullet+}$-$C_{60}^{\bullet-}$) and BET from $C_{60}^{\bullet-}$ to $H_2BCh^{\bullet+}$ is slower than the intersystem crossing as shown in Scheme 3a. In contrast to the case of H_2BCh-C_{60}, the BET from $C_{60}^{\bullet-}$ to $ZnCh^{\bullet+}$ in $ZnCh^{\bullet+}$-$C_{60}^{\bullet-}$ generates the ground-state rather than the triplet excited state, since the triplet excited state is higher in energy than the radical ion pair (Scheme 3b).[35] The long lifetime of $ZnCh^{\bullet+}$-$C_{60}^{\bullet-}$ indicates that the back electron transfer is deeply in the Marcus inverted region where the electron-transfer rate decreases with increasing the driving force. This is the reason the back electron transfer in $ZnCh^{\bullet+}$-$C_{60}^{\bullet-}$ generates the ground state rather than the triplet excited state.

Driving Force Dependence of Electron Transfer. To quantify the driving force dependence on the ET rate constants (k_{ET}), eq 1 was employed,

$$k_{ET} = \left(\frac{4\pi^3}{h^2 \lambda\, k_B T}\right)^{1/2} V^2 \exp\left(-\frac{(\Delta G^0_{ET} + \lambda)^2}{4\lambda\, k_B T}\right) \qquad (1)$$

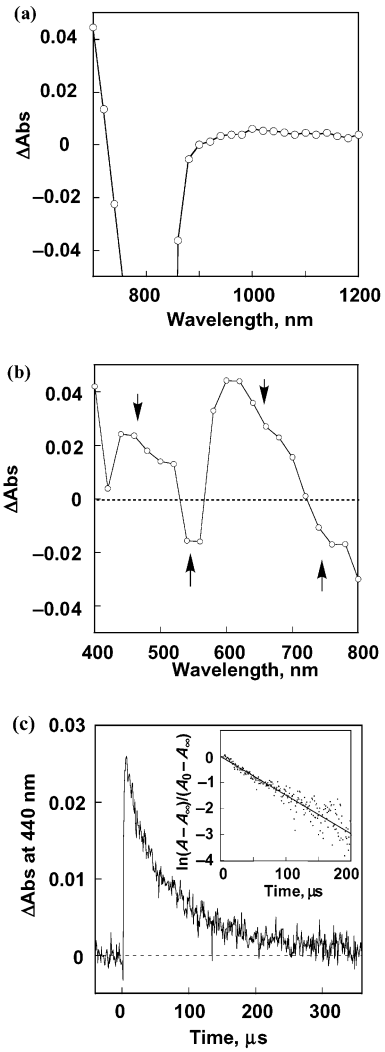

Figure 4. (a) Transient absorption spectrum of H_2BCh-C_{60} (**1**) (1.0×10^{-4} M) in deaerated PhCN at 298 K observed at (a) 700−1200 nm and (b) 400−800 nm taken at 0.1 μs after laser excitation at 355 nm, (c) the decay profile at 440 nm. Inset: first-order plot.

where V is the electronic coupling matrix element, k_B is the Boltzmann constant, h is the Planck constant, and T is the absolute temperature.[15] Figure 5 shows a plot of log k_{ET} or k_{BET} vs $-\Delta G^0_{ET}$, $-\Delta G^0_{BET}$ for the dyads **1** and **2** together with the data reported previously for the dyads (**5**−**8**). The best fit of eq 1 provides $\lambda = 0.51$ eV and $V = 7.8$ cm^{-1}. On the other hand, for the zinc porphyrin linked fullerene dyad with a longer amide linkage (ZnP−CONH−C_{60}, **9**),[14a] the driving force dependence is also plotted in Figure 5.

The photoinduced ET processes in the dyads are located in the normal region of the Marcus parabola ($\Delta G^0_{ET} > -\lambda$), whereas the BET process from $C_{60}^{\bullet-}$ to $ZnCh^{\bullet+}$ is in the inverted region ($\Delta G^0_{BET} < -\lambda$). In the inverted region, the k_{BET} value decreases with decreasing λ value. The solvent reorganization energy is expected to decrease with decreasing the donor−acceptor distance. Thus, the small λ value (0.51 eV) in the present dyad systems with the short spacers leads to the small k_{BET} value as compared to the value of any other D−A dyad system containing a porphyrin, chlorin, or bacteriochlorin as the donor and C_{60} as the acceptor.[23]

The λ value (0.51 eV) in the present dyad systems is smaller than the value (0.66 eV) reported for ZnP−CONH−C_{60} (**9**) with an edge-to-edge distance (R_{ee}) of 11.9 Å.[14] The R_{ee} value between ZnCh and C_{60} in the dyad (**2**) is evaluated as 5.9 Å

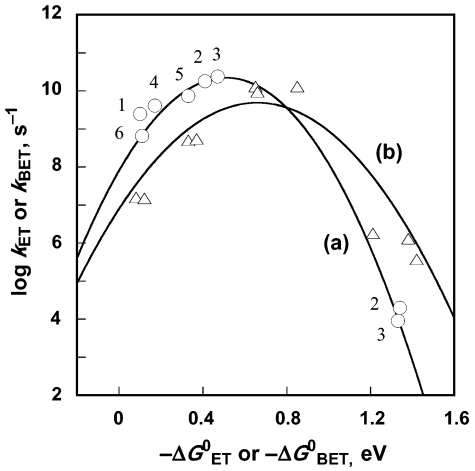

Figure 5. Driving force ($-\Delta G^0_{ET}$ or $-\Delta G^0_{BET}$) dependence of intramolecular ET rate constants (k_{ET} or k_{BET}) in (a) C_{60}-linked dyads in PhCN (○) and (b) ZnP−CONH−C_{60} (△).[14a] The curves represent the best fit to eq 1; (a) $\lambda = 0.51$ eV and $V = 7.8$ cm^{-1} and (b) $\lambda = 0.66$ eV and $V = 3.9$ cm^{-1}. Numbers refer to compounds in Table 2.

SCHEME 3

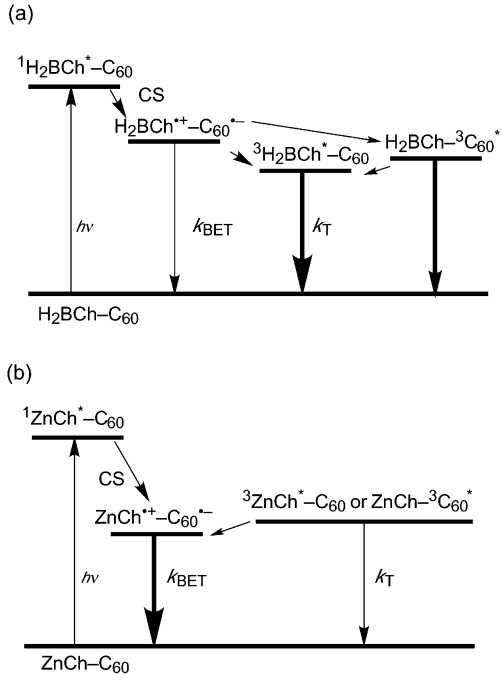

from the optimized structure that was calculated by the PM3 method. The smaller R_{ee} value in the present system may result in the smaller solvent reorganization energy as compared to the zinc tetraphenylporphyrin-C_{60} dyad system, since the smaller the R_{ee}, the smaller will be the solvent reorganization energy, as expected from the Marcus theory of electron transfer.[15] The solvent reorganization in ET of C_{60} and porphyrins is known to play a major role in determining the overall λ value, which includes a small reorganization energy of the inner coordination spheres associated with the little structural change in ET of C_{60} and porphyrins. The smaller R_{ee} value also results in the larger V value (6.8 cm^{-1}) as compared to the value (3.9 cm^{-1}) of the ZnP−CONH−C_{60} (**9**) with a larger R_{ee} value.

In summary, we have successfully shown the Marcus parabolic dependence of the logarithm of ET rate constants on the driving force. The extremely small reorganization energy is obtained in the electron transfer of the fullerene-based dyad with short linkage system. Relatively long-lived charge-separated states can be achieved in zinc chlorin-C_{60} dyads with a short linkage without the loss of excitation energy. This study has provided an important strategy to obtain the charge-separated state which has not only a high energy but also a long lifetime.

Acknowledgment. We thank the Ministry of Education, Culture, Sports, Science and Technology, Japan for a grant in aid (13440216), the Robert A. Welch Foundation (K.M.K., Grant E−680) for financial support, and the shared resources of the Roswell Park Cancer Center Support Grant (P30CA16056). Mass spectrometry analyses were performed at the Mass Spectrometry facility, Michigan State University, East Lansing, Michigan.

Supporting Information Available: Transient absorption spectrum of ZnCh-C_{60} (**2**) at NIR region (S1), ESR spectrum measured at 143 K of the photoirradiated dyad ZnCh-C_{60} (**2**) with a high-pressure mercury lamp (S2). This material is available free of charge via the Internet at http://pubs.acs.org.

References and Notes

(1) (a) Imahori, H.; Sakata, Y. *Adv. Mater.* **1997**, *9*, 537. (b) Imahori, H.; Sakata, Y. *Eur. J. Org. Chem.* **1999**, *2445*, 5. (c) Guldi, D. M. *Chem. Commun.* **2000**, 321. (d) Guldi, D. M.; Prato, M. *Acc. Chem. Res.* **2000**, *33*, 695. (e) Fukuzumi, S.; Guldi, D. M. In *Electron Transfer in Chemistry*; Balzani, V. Ed.; Wiley-VCH: Weinheim, 2001; Vol. 2, pp 270−337.

(2) Fukuzumi, S.; Imahori, H. In *Electron Transfer in Chemistry*; Balzani, V., Ed.; Wiley-VCH: Weinheim, 2001; pp 927−975.

(3) Guldi, D. M.; Kamat, P. V. In *Fullerenes, Chemistry, Physics, and Technology*; Kadish, K. M., Ruoff, R. S., Eds.; Wiley-Interscience: New York, 2000; pp 225−281.

(4) (a) Gust, D.; Moore, T. A. In *The Porphyrin Handbook*; Kadish, K. M., Smith, K. M., Guilard, R., Eds.; Academic Press: San Diego, CA, 2000; Vol. 8, pp 153−190. (b) Gust, D.; Moore, T. A.; Moore, A. L. *Res. Chem. Intermed.* **1997**, *23*, 621. (c) Gust, D.; Moore, T. A.; Moore, A. L. *Acc. Chem. Res.* **2001**, *34*, 40.

(5) (a) Martín, N.; Sánchez, L.; Illescas, B.; Pérez, I. *Chem. Rev.* **1998**, *98*, 2527. (b) Diederlich, F.; Gómez-López, M. *Chem. Rev. Soc.* **1999**, *28*, 263.

(6) (a) Jensen, A. W.; Wilson, S. R.; Schuster, D. I. *Bioorg. Med. Chem.* **1996**, *4*, 767. (b) Schuster, D. I.; Cheng, P.; Wilson, S. R.; Prokhorenko, V.; Katterle, M.; Holzwarth, A. R.; Braslavsky, S. E.; Klihm, G.; Williams, R. M.; Luo, C. *J. Am. Chem. Soc.* **1999**, *121*, 11599. (c) Wilson, S. R.; Schuster, D. I.; Nuber, B.; Meier, M. S.; Maggini, M.; Prato, M.; Taylor, R. In *Fullerenes*; Kadish, K. M., Ruoff, R. S., Eds.; John Wiley & Sons: New York, 2000; Chapter 3, pp 91−176.

(7) Sun, Y.-P.; Riggs, J. E.; Guo, Z.; Rollins, H. W. In *Optical and Electronic Properties of Fullerenes and Fullerene-Based Materials*; Shinar, J., Vardeny, Z. V., Kafafi, Z. H., Eds.; Marcel Dekker: New York, 2000; pp 43−81.

(8) (a) Bell, T. D. M.; Smith, T. A.; Ghiggino, K. P.; Ranasinghe, M. G.; Shephard, M. J.; Paddon-Row, M. N. *Chem. Phys. Lett.* **1997**, *268*, 223. (b) Guldi, D. M.; Luo, C.; Prato, M.; Dietel, E.; Hirsch, A. *Chem. Commun.* **2000**, 373.

(9) (a) Kurreck, H.; Huber, A. *Angew. Chem.* **1995**, *107*, 929; *Angew. Chem., Int. Ed. Engl.* **1995**, *34*, 849. (b) Gust, D.; Moore, T. A. *Adv. Photochem.* **1991**, *16*, 1. (c) Gust, D.; Moore, T. A. *Top. Curr. Chem.* **1991**, *159*, 103. (d) Wasielewski, M. R. *Chem. Rev.* **1992**, *92*, 435.

(10) (a) Wasielewski, M. R.; Gaines, G. L., III; Wiederrecht, G. P.; Svec, W. A.; Niemczyk, M. P. *J. Am. Chem. Soc.* **1993**, *115*, 10442. (b) Johnson, D. G.; Niemczyk, M. P.; Minsek, D. W.; Wiederrecht, G. P.; Svec, W. A.; Gaines, G. L., III; Wasielewski, M. R. *J. Am. Chem. Soc.* **1993**, *115*, 5692.

(11) (a) Prato, M. *J. Mater. Chem.* **1997**, *7*, 1097.

(12) (a) Imahori, H.; Hagiwara, K.; Akiyama, T.; Aoki, M.; Taniguchi, S.; Okada, T.; Shirakawa, M.; Sakata, Y. *Chem. Phys. Lett.* **1996**, *263*, 545. (b) Tkachenko, N. V.; Guenther, C.; Imahori, H.; Tamaki, K.; Sakata, Y.; Fukuzumi, S.; Lemmetyinen, H. *Chem. Phys. Lett.* **2000**, *326*, 344. (c) Imahori, H.; Tamaki, K.; Yamada, H.; Yamada, K.; Sakata, Y.; Nishimura, Y.; Yamazaki, I.; Fujitsuka, M.; Ito, O. *Carbon* **2000**, *38*, 1599. (d) Imahori, H.; Tkachenko, N. V.; Vehmanen, V.; Tamaki, K.; Lemmetyinen, H.; Sakata, Y.; Fukuzumi, S. *J. Phys. Chem. A* **2001**, *105*, 1750. (e) Vehmanen, V.; Tkachenko, N. V.; Imahori, H.; Fukuzumi, S.; Lemmetyinen, H. *Spectrochim. Acta, Part A* **2001**, *57*, 2229. (f) Imahori, H.; Yamada, H.; Guldi, D. M.; Endo, Y.; Shimomura, A.; Kundu, S.; Yamada, K.; Okada, T.; Sakata, Y.; Fukuzumi, S. *Angew. Chem., Int. Ed.* **2002**, *42*, 2344.

(13) Guldi, D. M.; Asmus, K.-D. *J. Am. Chem. Soc.* **1997**, *119*, 5744.

(14) (a) Imahori, H.; Tamaki, K.; Guldi, D. M.; Luo, C.; Fujitsuka, M.; Ito, O.; Sakata, Y.; Fukuzumi, S. *J. Am. Chem. Soc.* **2001**, *123*, 2607. (b) Luo, C.; Guldi, D. M.; Imahori, H.; Tamaki, K.; Sakata, Y. *J. Am. Chem. Soc.* **2000**, *122*, 6535. (c) Yamada, K.; Imahori, H.; Nishimura, Y.; Yamazaki, I.; Sakata, Y. *Chem. Lett.* **1999**, 895.

(15) (a) Marcus, R. A. *Annu. Rev. Phys. Chem.* **1964**, *15*, 155. (b) Marcus, R. A.; Sutin, N. *Biochim. Biophys. Acta* **1985**, *811*, 265. (c) Marcus, R. A. *Angew. Chem., Int. Ed. Engl.* **1993**, *32*, 1111.

(16) Imahori, H.; Guldi, D. M.; Tamaki, K.; Yoshida, Y.; Luo, C.; Sakata, Y.; Fukuzumi, S. *J. Am. Chem. Soc.* **2001**, *123*, 6617.

(17) Scheer, H.; Inhoffen, H. H. In *The Porphyrins*; Dolphin, D., Ed.; Academic Press: New York, 1978; Vol II, pp 45−90.

(18) Hanson, L. S. In *Chlorophylls*; Scheer, H., Ed.; CRC Press: Boca Raton, FL, 1991; pp 993−1014. (b) Plato, M.; Möbius, K.; Lubitz, W. In *Chlorophylls*; Scheer, H., Ed.; CRC Press: Boca Raton, FL, 1991; pp 1015−1046.

(19) Fukuzumi, S.; Ohkubo, K.; Chen, Y.; Pandey, R. K.; Zhan, R.; Shao, J.; Kadish, K. M. *J. Phys. Chem. A* **2002**, *106*, 5105.

(20) (a) Helaja, J.; Tauber, A. Y.; Abel, Y.; Tkachenko, N. V.; Lemmetyinen, H.; Kilpeläinen, I.; Hynninen, P. H. *J. Chem. Soc., Perkin Trans. 1* **1999**, 2403. (b) Tkachenko, N. V.; Rantala, L.; Tauber, A. Y.; Helaja, J.; Hynninen, P. H.; Lemmetyinen, H. *J. Am. Chem. Soc.* **1999**, *121*, 9378. (c) Tkachenko, N. V.; Vuorimaa, E.; Kesti, T.; Alekseev, A. S.; Tauber, A. Y.; Hynninen, P. H.; Lemmetyinen, H. *J. Phys. Chem. B* **2000**, *104*, 6371.

(21) Zheng, G.; Dougherty, T. J.; Pandey, R. K. *Chem. Commun.* **1999**, 2469.

(22) (a) Kutzki, O.; Walter, A.; Montforts, F.-P. *Helv. Chim. Acta* **2000**, *83*, 2231. (b) Montforts, F.-P.; Kutzki, O. *Angew. Chem., Int. Ed.* **2000**, *39*, 599. (c) Smirnov, S.; Vlassiouk. I.; Kutzki, O.; Wedel, M.; Montforts, F.-P. *J. Am. Chem. Soc.* **2002**, *124*, 4212.

(23) Fukuzumi, S.; Ohkubo, K.; Imahori, H.; Shao, J.; Ou, Z.; Zheng, G.; Chen, Y.; Pandey, R. K.; Fujitsuka, M.; Ito, O.; Kadish, K. M. *J. Am. Chem. Soc.* **2001**, *123*, 10676.

(24) Perrin, D. D.; Armarego, W. L. F. *Purification of Laboratory Chemicals*; Butterworth-Heinemann: Oxford, 1988.

(25) For the cyclic voltammograms of C_{60} in PhCN, see: Dubois, D.; Moninot, G.; Kutner, W.; Jones, M. T.; Kadish, K. M. *J. Phys. Chem.* **1992**, *96*, 7137.

(26) Reed, C. A.; Bolskar, R. D. *Chem. Rev.* **2000**, *100*, 1075.

(27) The origin of the initial fast decay component is not clear at present. Since the fast decay component is rather minor, the rate is determined from the major decay component.

(28) (a) Fukuzumi, S.; Suenobu, T.; Patz, M.; Hirasaka, T.; Itoh, S.; Fujitsuka, M.; Ito, O. *J. Am. Chem. Soc.* **1998,** *120*, 8060. (b) Fukuzumi, S.; Suenobu, T.; Hirasaka, T.; Sakurada, N.; Arakawa, R.; Fujitsuka, M.; Ito, O. *J. Phys. Chem. A* **1999**, *103*, 5935.

(29) The Coulombic interaction is neglected to evaluate the $-\Delta G^0_{ET}$ value in a polar solvent such as PhCN.

(30) Imahori, H.; El-Khouly, M. E.; Fujitsuka, M.; Ito, O.; Sakata, Y.; Fukuzumi, S. *J. Phys. Chem. A* **2001**, *105*, 325.

(31) (a) Kadish, K. M.; Gao, X.; Van Caemelbecke, E.; Suenobu, T.; Fukuzumi, S. *J. Phys. Chem. A* **2000**, *104*, 3878. (b) Guldi, D. M.; Asmus, K.-D. *J. Phys. Chem. A* **1997**, *101*, 1472. (c) Guldi, D. M.; Hungerbühler, H.; Asmus, K.-D. *J. Phys. Chem.* **1995**, *99*, 9380.

(32) Anderson, J. L.; An, Y.-Z.; Rubin, Y.; Foote, C. S. *J. Am. Chem. Soc.* **1994**, *116*, 9763.

(33) For the *g* values of ESR spectra of C_{60} derivatives, see: Fukuzumi, S.; Mori, H.; Suenobu, T.; Imahori, H.; Gao, X.; Kadish, K. M. *J. Phys. Chem. A* **2000**, *104*, 10688.

(34) Although the energy of the radical ion pair of $H_2BCh^{\bullet+}$-$C_{60}^{\bullet-}$ (1.35 eV) is comparable to that of $ZnCh^{\bullet+}$-$C_{60}^{\bullet-}$ (1.36 eV), the excitation energy of H_2BCh is significantly lower than that of ZnCh as indicated by the large red-shift of the Q_y band (824 nm) as compared to ZnCh (683 nm).[19]

(35) The electron-transfer pathway from $^1C_{60}$* is omitted in Scheme 3b, since this is a minor pathway as compared to that from ^{1}ZnCh* (vide supra).